Edge States and Topological Phases in One-Dimensional Optical Superlattices

Li-Jun Lang, Xiaoming Cai, and Shu Chen*

Beijing National Laboratory for Condensed Matter Physics, Institute of Physics, Chinese Academy of Sciences, Beijing 100190, China

(Received 31 October 2011; published 29 May 2012)

We show that one-dimensional quasiperiodic optical lattice systems can exhibit edge states and topological phases which are generally believed to appear in two-dimensional systems. When the Fermi energy lies in gaps, the Fermi system on the optical superlattice is a topological insulator characterized by a nonzero topological invariant. The topological nature can be revealed by observing the density profile of a trapped fermion system, which displays plateaus with their positions uniquely determined by the ration of wavelengths of the bichromatic optical lattice. The butterflylike spectrum of the superlattice system can be also determined from the finite-temperature density profiles of the trapped fermion system. This finding opens an alternative avenue to study the topological phases and Hofstadter-like spectrum in one-dimensional optical lattices.

DOI: 10.1103/PhysRevLett.108.220401 PACS numbers: 05.30.Fk, 03.75.Hh, 73.21.Cd

Introduction.—In recent years ultracold atomic systems have proven to be powerful quantum simulators for investigating various interesting physical problems including many-body physics [1] and topological insulators [2]. In comparison with traditional condensed matter systems, cold-atom systems provide more control in constructing specific optical lattice Hamiltonians by allowing both tunable hopping and trapping potential to be adjusted as needed; thus, optical lattices populated with cold atoms offer a very promising alternative avenue to build topological insulating states [2]. Several schemes exploring topological insulators with or without Landau levels in optical lattices have been proposed [3–6]. So far all these schemes focus on two-dimensional (2D) systems, as one-dimensional (1D) systems without additional symmetries are generally thought to lack topological nontrivial phases [7].

In this work, we study properties of trapped fermions on 1D quasiperiodic optical lattices and show that these systems display nontrivial topological properties, which share the same physical origins of topological phases of 2D quantum Hall effects on periodic lattices [8]. The quasiperiodic optical lattices can be generated by superimposing two 1D optical lattices with commensurate or incommensurate wavelengths [9–11], which has led to the experimental observation of Anderson localization of a noninteracting Bose-Einstein condensate of ^{39}K atoms in 1D incommensurate optical lattices [10]. Motivated by the experimental progress, one-dimensional optical superlattices have been theoretically studied [12–16]. For a quasiperiodic superlattice, the single-particle spectrum is organized in bands. When fermions are loaded in the superlattice, the system shall form insulators if the chemical potential (Fermi energy) lies in the gaps. For the open boundary system, localized edge states are found to appear in the gap regimes. The appearance of edge states is a signature indicating that the bulk states are topological insulators characterized by a nonzero Chern number. We show that the topological invariant Chern number can be detected from the density distribution of a trapped fermion system, which displays plateaus in the local average density profiles with positions of plateaus uniquely determined by the ration of wavelengths of the bichromatic optical lattice. Through the analysis of universal scaling behaviors in quantum critical regimes of conductor-to-insulator transitions, we further display that both the positions and widths of plateaus can be read out from the finite-temperature density distributions, which provides us with an alternative way to study topological phases and a Hofstadter-like spectrum by using 1D optical superlattices. We notice that localized boundary states in 1D incommensurate lattices have been experimentally observed very recently by using photonic quasicrystals [17].

Quasiperiodic lattices.—We consider a 1D polarized Fermi gas loaded in a bichromatic optical lattice [10,11], which is described by

$$H = -t\sum_i (\hat{c}_i^\dagger \hat{c}_{i+1} + \text{H.c.}) + \sum_{i=1}^{L} V_i \hat{n}_i, \tag{1}$$

with

$$V_i = V\cos(2\pi\alpha i + \delta), \tag{2}$$

where L is the number of the lattice sites, $\hat{c}_i^\dagger$ ($\hat{c}_i$) is the creation (annihilation) operator of the fermion, and $\hat{n}_i = \hat{c}_i^\dagger \hat{c}_i$. The hopping amplitude t is set to be the unit of the energy ($t = 1$), and V is the strength of the commensurate (incommensurate) potential with α being a rational (irrational) number and δ an arbitrary phase whose effect shall be illustrated later. Suppose that the nth eigenstate of a single particle in the 1D lattice is given by $|\psi_n\rangle = \sum_i u_{i,n} c_i^\dagger |0\rangle$, the eigenvalue equation $H|\psi_n\rangle = E_n|\psi_n\rangle$ leads to the following Harper equation:

$$-(u_{i+1,n} + u_{i-1,n}) + V\cos(2\pi\alpha i + \delta)u_{i,n} = E_n u_{i,n}, \quad (3)$$

where $u_{i,n}$ is the amplitude of the particle wave function at the ith site with V_i the on-site diagonal potential and E_n the nth single particle eigenenergy. The ground state wave function of the N spinless free fermionic system can be written as $|\Psi_F^G\rangle = \prod_{n=1}^{N}\sum_{i=1}^{L} u_{i,n}c_i^\dagger|0\rangle$, where N is the number of fermions.

The solution to Eq. (3) is closely related to the structure of the potential V_i. For the incommensurate case $V_i = V\cos(2\pi\alpha i)$ with irrational α, Eq. (3) is the well-known Aubry-André model [18], which showed that when $V < 2$ all the single particle states are extended and when $V > 2$ all the single particle states are the localized states. However, for a periodic V_i, all the single particle states are extended band states according to Bloch's theorem. Next we shall consider the commensurate potential V_i with a rational α given by $\alpha = p/q$ with p and q being integers which are prime to each other. Since the potential V_i is periodic with a period q, the wave functions take the Bloch form, which fulfills $u_{i+q} = e^{ikq}u_i$, for the lattice under the periodic boundary condition. Taking $u_j = e^{ikj}\phi_j(k)$ for $|k| \le \pi/q$, we have $\phi_{j+q}(k) = \phi_j(k)$. In terms of $\phi_j(k)$, Eq. (3) becomes

$$-[e^{ik}\phi_{j+1} + e^{-ik}\phi_{j-1}] + V\cos(2\pi jp/q + \delta)\phi_j = E(k)\phi_j. \quad (4)$$

Since $\phi_{j+q} = \phi_j$, the problem of solving the Harper equation, Eq. (4), reduces to solving the eigenvalue equation, $M\Phi = E\Phi$, where $\Phi = (\phi_1, \ldots, \phi_q)^T$ and M is a $q \times q$ matrix. Solving the eigenvalue problem, we get q eigenvalues: $E_\alpha(k)$ with $\alpha = 1, \ldots, q$. Consequently, the energy spectrum consists of q bands. As an example, the energy spectrum for a commensurate lattice with $\alpha = 1/3$ and $L = 99$ under periodic boundary condition is given in Fig. 1(a). For the lattice with an open boundary condition, the momentum k is no longer a good quantum number. There appear edge states in gap regimes as indicated by "star" symbols of located at gap regimes in Fig. 1(b). As shown in Fig. 1(c), these edge states are localized in the left and right boundaries in contrast to extended states marked by "plus" symbols of in band regimes.

As the phase δ varies from 0 to 2π, the spectrum for a given $\alpha = p/q$ changes periodically. The position of the edge states in the gaps also varies continuously with the change of δ. In Fig. 2, we show the spectrum of the quasiperiodic systems with $\alpha = 1/3$ and $1/4$ versus δ under the open boundary condition. The shade regimes correspond to the band regimes and the lines between bands are the spectra of edge states.

Topological invariant.—The appearance of edge states is generally attributed to the nontrivial topological properties of bulk systems [2,19]. Next we explore the topological properties of states under the periodic boundary condition.

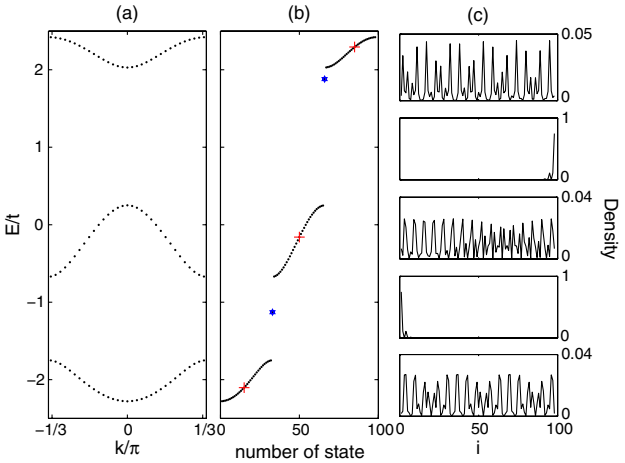

FIG. 1 (color online). Spectrum of Hamiltonian (1) with $\alpha = 1/3$, $V = 1.5$, and $\delta = 2\pi/3$. (a) Energy bands for the system with 99 sites under periodic boundary conditions. (b) Eigenenergies in ascending order for the system with 98 sites under open boundary conditions. (c) From top to bottom, the figures represent the wave functions of states marked by labels (plus signs for states in bands and stars for states in gaps) in (b).

The topological property of the system can be understood in terms of the Berry phase in k space, which is defined as $\gamma = \oint A_k dk$, where A_k is the Berry connection $A_k = i\langle\phi(k)|\partial_k|\phi(k)\rangle$ and $\phi(k)$ the occupied Bloch state [20]. Adiabatically varying the phase δ from 0 to 2π, we get a manifold of Hamiltonian $H(\delta)$ in the space of parameter δ. Similarly, we can define the Berry connection $A_\delta = i\langle\phi(k,\delta)|\partial_\delta|\phi(k,\delta)\rangle$. For eigenstates $\phi(k,\delta)$ of $H(\delta)$, we may use the Chern number to characterize their topological properties. The Chern number is a

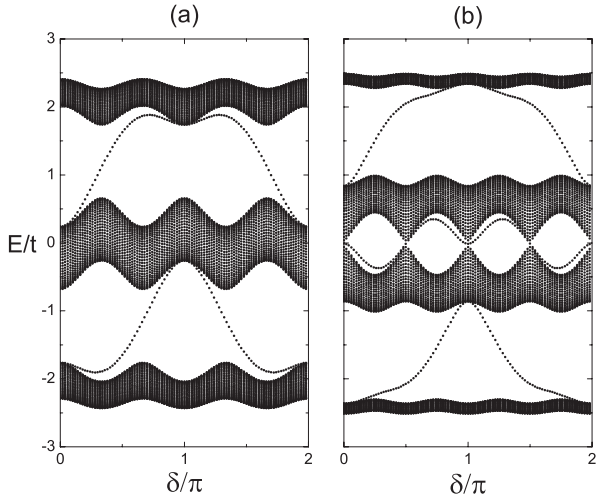

FIG. 2. Energies varying with the phase δ for systems with $V = 1.5$, (a) $\alpha = 1/3$, $L = 98$, and (b) $\alpha = 1/4$, $L = 99$ under open boundary conditions.

topological invariant which can be calculated via $C = \frac{1}{2\pi}\int_0^{2\pi/q} dk \int_0^{2\pi} d\delta[\partial_k A_\delta - \partial_\delta A_k]$. To calculate it, we need work on a discretized Brillouin zone. Here we follow the method in Ref. [21] to directly perform the lattice computation of the Chern number. For the system with $\alpha = 1/3$, we find that the Chern number for fermions in the lowest filled band (with 1/3 filling) is 1, while the Chern number for states with the second band fully filled (with 2/3 filling) is -1.

To understand the topological origin of fermions in the 1D quasiperiodic lattices, we explore the connection of the present model to the well-known Hofstadter problem [8,22], which describes electrons hopping on a 2D square lattice in a perpendicular magnetic field, with the Hamiltonian given by $H = -\sum_{\langle i,j\rangle} t_{ij}\hat{c}_j^\dagger \hat{c}_i e^{i2\pi\phi_{ij}}$, where the summation is over nearest-neighbor sites and the magnetic flux through each plaquette given by $\phi = \sum_{\text{plaquette}} \phi_{ij}$. Taking the Landau gauge, the eigenvalue problem is described by the Harper equation [8]: $-t_x(\psi_{j-1} + \psi_{j+1}) - 2t_y \cos(2\pi j\phi - k_y)\psi_j = E(k_y)\psi_j$, where t_x (t_y) is the hopping amplitude along the x (y) direction. If we make substitutions of $t \to t_x$, $V \to -2t_y$, $\alpha \to \phi$, and $\delta \to -k_y$, the current 1D problem can be mapped to the lattice version of the 2D integer Hall effect problem. For the latter case, it was shown that when the chemical potential lies in gap regimes, the Hall conductance of the system is quantized [23] and the corresponding Hofstadter insulating phase is a topological insulator characterized by a nonzero Chern number.

Keeping this connection in mind, it is not strange to see that the energy spectrum of the 1D quasiperiodic system versus different α has a similar structure as the spectrum of the 2D Hofstadter butterfly. In Figs. 3(a) and 3(b), we show the spectrum for the system with phase $\delta = 0$ and $\delta = \pi/4$, respectively. The basic structure is quite similar for different phases except for some minor differences, for example, the spectrum for $\alpha = \pi/4$ is continuous around $E = 0$ for $\delta = 0$, but separated for $\delta = \pi/4$ [see also Fig. 2(b)]. The familiar Hofstadter spectrum is actually a summation over all the 1D spectra with different phases δ from 0 to 2π. Despite the existence of the mapping between the 1D quasiperiodic system and the 2D Hofstadter system, we note that the edge modes in the 1D system are localized and would not be used for dissipationless transport as in high-dimensional systems.

Experimental detection.—In realistic ultracold atom experiments, we need to consider the effect of an external confining potential; i.e., V_i in Eq. (1) is given by

$$V_i = V\cos(\alpha 2\pi i + \delta) + V_H(i - i_0)^2, \tag{5}$$

where V_H is the strength of the additional harmonic trap with i_0 being the position of trap center. The density distribution for the trapped system can be calculated via $n_i = \langle\Psi_F^G|\hat{n}_i|\Psi_F^G\rangle$ with Ψ_F^G the ground state wave function. In Fig. 4, we have shown the local average density distribution of fermions trapped in both commensurate and incommensurate optical lattices with a harmonic trap. Here, in order to reduce the oscillations in density profiles induced by the modulation of potentials, we have defined the local average density $\bar{n}_i = \sum_{j=-M}^{M} n_{i+j}/(2M+1)$, where $2M+1$ is the length to count the local average density with $M \ll L$ [24]. After counting on the locations of plateaus, we find that the heights of plateaus are completely decided by α with values $\bar{n}(\alpha) = \alpha$, $1-\alpha, 2\alpha, 1-2\alpha, 4\alpha, 1-4\alpha, \ldots$, if the values are in the range of (0,1). The plateaus with $\bar{n}_i = \alpha$, $1-\alpha$ are the widest ones corresponding to the largest gap regimes in the butterfly spectrum, while $\bar{n}_i = 2\alpha$, $1-2\alpha$ correspond

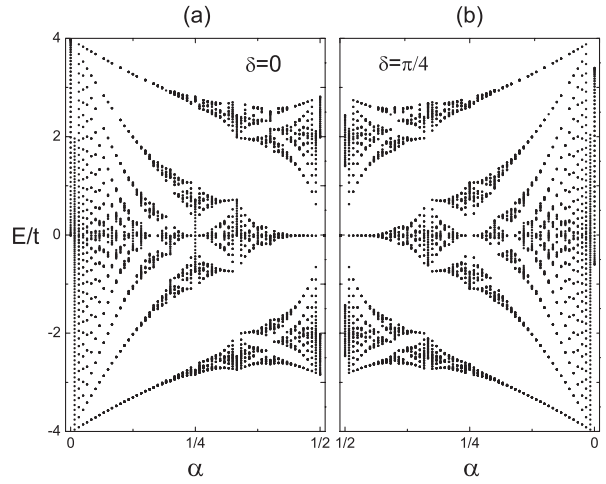

FIG. 3. The butterflylike energy spectra with respect to α varying from 0 to 1/2 with different phases: (a) $\delta = 0$, (b) $\delta = \pi/4$. Both figures are for the system with $V = 2$ and $L = 120$ under periodic boundary conditions.

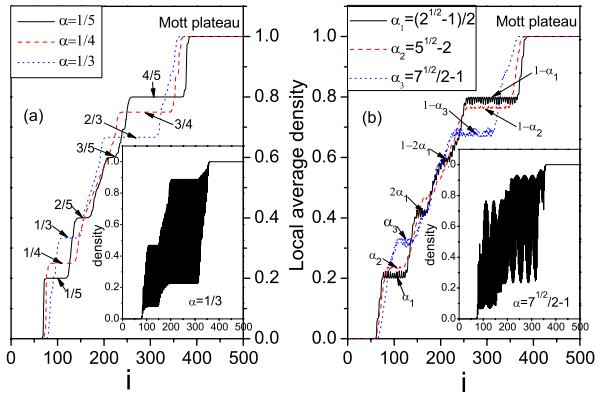

FIG. 4 (color online). The local average density profiles for systems with rational α (a) and irrational α (b). Inserts for both pictures are the corresponding density profiles. The system is with 1000 sites, 600 free fermions, $V = 1.5$, $\delta = 0$, and $V_H = 3 \times 10^{-5}$. Here we take $M = q$ for the rational case of (a) and $M = 20$ for the irrational case of (b).

to the smaller gap regimes. The width of plateau is associated with the size of gap.

One can also understand the appearance of plateaus under the local-density approximation (LDA), in which a local chemical potential is defined as $\mu(i) = \mu - V_H(i)$, where $V_H(i)$ is the harmonic trap potential and μ is determined by $\sum_i n[\mu(i), T] = N$. The LDA is applicable provided that the number of fermions is large, and the variation of the trap potential is slow. Within the LDA, the local chemical potential $\mu(i)$ decreases parabolically away from the center of the trap. When the local chemical potential lies in one of the gaps, there appear plateaus in the density profile. The discernible number of plateaus is related to the size of the energy gaps. For instance, in Fig. 4, the plateau with $n = 1$ corresponds to the band insulator with a completely filled band, which is topologically trivial with the zero Chern number. For $\alpha = 1/3$, the chemical potential passes through two gap regions which produces two plateaus with $n = 1/3$ and $n = 2/3$, whereas for $\alpha = 1/5$ the chemical potential passes through four gap regions which gives four plateaus with $n = 1/5, 2/5, 3/5, 4/5$, respectively. The Chern number can be obtained from the density by using the Streda formula [3,25], which is valid when the chemical potential lies in a gap. From the Streda formula $C = \frac{\partial \bar{n}(\alpha)}{\partial \alpha}$, we can get $C = 1, -1$ for $\bar{n}_i = \alpha, 1 - \alpha$ and $C = 2, -2$ for $\bar{n}_i = 2\alpha, 1 - 2\alpha$.

In principle, all gaps in the spectrum, including the nontrivial smaller gaps in the butterfly, can be determined via observing the corresponding plateaus. The widths of plateaus are proportional to the sizes of corresponding energy gaps. Experimentally, it becomes increasingly harder to observe these smaller gaps, as the corresponding plateaus are very narrow, which needs a more precisely experimental measurement of the density distribution. For the realistic detection, we need to consider the effect of temperature. The finite-temperature density distribution can be calculated via $n_i(T) = \frac{1}{Z}\sum_{n=1}^{N_s} e^{-E_n/k_BT}\langle\Psi_F^n|\hat{c}_i^\dagger\hat{c}_i|\Psi_F^n\rangle$, where $N_s = L!/(L-N)!N!$ is the number of states, E_n is the energy of eigenstate Ψ_F^n, and $Z = \sum_{n=1}^{N_s} e^{-E_n/k_BT}$ is the canonical partition function [26]. In Fig. 5(a), we display the local average density profiles at different temperatures. It is shown that plateaus already become invisible for $T > 0.3t$. Despite the fact that the obvious plateaus are smeared out by temperature fluctuations, we demonstrate that the position and the width of zero-temperature plateaus can be uniquely mapped out from finite-temperature density distributions of the trapped optical lattice system, which fulfill some universal scaling relations [27] near the zero-temperature phase transition point $\mu = \mu_c$:

$$n(\mu, T) - n_r(\mu, T) = T^{(d/z)+1-(1/\nu z)}\Omega\left(\frac{\mu - \mu_c}{T^{1/\nu z}}\right), \quad (6)$$

where $n = n(T, \mu)$ represents the density distribution for fermions with temperature T and chemical potential μ,

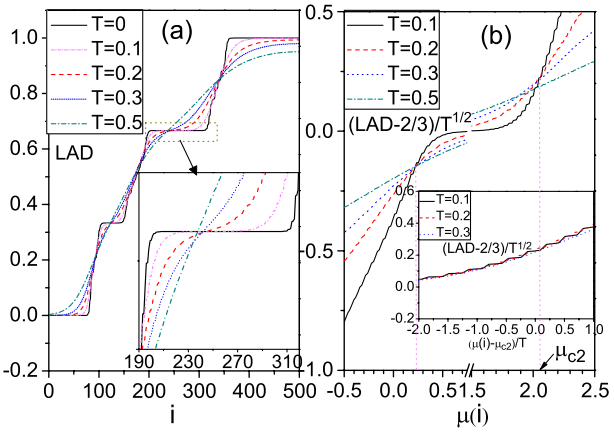

FIG. 5 (color online). (a): Local average density profiles for systems with different temperatures. Insert: Enlargement of the plateau area. (b): Scaled local average density profiles vs $\mu(i)$ at different temperatures. Insert: The universal function around critical point μ_{c_2} for the corresponding system. The system is with 1000 sites, 600 free fermions, $V = 1.5$, $\alpha = 1/3$, $\delta = 0$, and $V_H = 3 \times 10^{-5}$.

$n_r(\mu, T)$ is the regular part of the density, $\Omega(x)$ is a universal function describing the singular part of density near criticality, $d = 1$ is the dimensionality of the system, ν is the correlation length exponent, and z is the dynamical exponent. It was shown that $z = 2$ and $\nu = 1/2$ for the metal-insulator transition of 1D free fermions [27]. From Fig. 5(b), we see that the different curves of $[\bar{n}(\mu, T) - 2/3]/T^{3/2}$ intersect at two points. From intersecting points, we can determine μ_{c_1} and μ_{c_2}, and thus the corresponding gap in the spectrum can be inferred from $\mu_{c_2} - \mu_{c_1}$. In terms of the scaled chemical potential $\tilde{\mu} = (\mu - \mu_c)/T$, curves for different temperatures collapse into a single one as shown in the inset of Fig. 5(b).

In order to connect to the real experiment in cold atoms, we refer to the parameters in Ref. [28] in which ^{40}K atoms were used in an optical lattice with spacing $a = 413$ nm, the deep of the potential $V_0 = 5E_R$, and the recoil energy $E_R = 45.98\hbar$ kHz; thus, the hopping magnitude $t = 0.066E_R = 3.035\hbar$ kHz. Correspondingly, the temperature T in Fig. 5 in unit t/k_B, where k_B is the Boltzmann constant, is of the order of 10 nK; e.g., $T = 0.1$ corresponds to 2.3084 nK.

Summary.—In summary, we explored the edge states and topological nature of Fermi systems confined in 1D optical superlattices. Our study reveals that the topological invariant can be detected from plateaus of density profiles of the trapped lattice systems. Our results also clarify the connection of 1D superlattice systems to 2D Hofstadter systems and will be useful for studying topological phases and observing the Hofstadter spectrum by using 1D optical lattices.

S. C. would thank Professor S. Q. Shen for helpful discussions on edge states of the dimerized chain which

stimulates our interest in the 1D topological insulator. This work has been supported by the NSF of China under Grants No. 11121063, No. 11174360, and No. 10974234, 973 grant, and the National Program for Basic Research of MOST.

Note added.—Recently we became aware of the experiment for the observation of edge states in 1D quasicrystals [17].

*schen@aphy.iphy.ac.cn

[1] I. Bloch, J. Dalibard, and W. Zwerger, Rev. Mod. Phys. **80**, 885 (2008).
[2] M. Z. Hasan and C. L. Kane, Rev. Mod. Phys. **82**, 3045 (2010); X.-L. Qi and S.-C. Zhang, Rev. Mod. Phys. **83**, 1057 (2011).
[3] R. O. Umucallar, H. Zhai, and M. Ö. Oktel, Phys. Rev. Lett. **100**, 070402 (2008).
[4] L. B. Shao, S.-L. Zhu, L. Sheng, D. Y. Xing, and Z. D. Wang, Phys. Rev. Lett. **101**, 246810 (2008).
[5] T. D. Stanescu, V. Galitski, and S. Das Sarma, Phys. Rev. A **82**, 013608 (2010).
[6] N. Goldman, I. Satija, P. Nikolic, A. Bermudez, M. A. Martin-Delgado, M. Lewenstein, and I. B. Spielman, Phys. Rev. Lett. **105**, 255302 (2010); B. Béri and N. R. Cooper, Phys. Rev. Lett. **107**, 145301 (2011).
[7] S. Ryu, A. P. Schnyder, A. Furusaki, and A. W. W. Ludwig, New J. Phys. **12**, 065010 (2010).
[8] D. R. Hofstadter, Phys. Rev. B **14**, 2239 (1976).
[9] L. Fallani, J. E. Lye, V. Guarrera, C. Fort, and M. Inguscio, Phys. Rev. Lett. **98**, 130404 (2007).
[10] G. Roati, C. D Errico, L. Fallani, M. Fattori, C. Fort, M. Zaccanti, G. Modugno, M. Modugno, and M. Inguscio, Nature (London) **453**, 895 (2008).
[11] B. Deissler, M. Zaccanti, G. Roati, C. D Errico, M. Fattori, M. Modugno, G. Modugno, and M. Inguscio, Nature Phys. **6**, 354 (2010).
[12] T. Roscilde, Phys. Rev. A **77**, 063605 (2008); Phys. Rev. A **82**, 023601 (2010).
[13] G. Roux, T. Barthel, I. P. McCulloch, C. Kollath, U. Schollwöck, and T. Giamarchi, Phys. Rev. A **78**, 023628 (2008); X. Deng, R. Citro, A. Minguzzi, and E. Orignac, Phys. Rev. A **78**, 013625 (2008).
[14] T. Yamashita, N. Kawakami, and M. Yamashita, Phys. Rev. A **74**, 063624 (2006).
[15] P. Buonsante, V. Penna, and A. Vezzani, Phys. Rev. A **70**, 061603 (2004).
[16] X. Cai, S. Chen, and Y. Wang, Phys. Rev. A **81**, 023626 (2010); Phys. Rev. A **81**, 053629 (2010).
[17] Y. E. Kraus, Y. Lahini, Z. Ringel, M. Verbin, and O. Zilberberg, arXiv:1109.5983.
[18] S. Aubry and G. André, Ann. Isr. Phys. Soc. **3**, 133 (1980).
[19] Y. Hatsugai, Phys. Rev. B **48**, 11851 (1993).
[20] D. Xiao, M.-C. Chang, and Q. Niu, Rev. Mod. Phys. **82**, 1959 (2010); R. Resta, Rev. Mod. Phys. **66**, 899 (1994).
[21] T. Fukui, Y. Hatsugai, and H. Suzuki, J. Phys. Soc. Jpn. **74**, 1674 (2005).
[22] P. G. Harper, Proc. Phys. Soc. London Sect. A **68**, 874 (1955).
[23] D. J. Thouless, M. Kohmoto, M. P. Nightingale, and M. den Nijs, Phys. Rev. Lett. **49**, 405 (1982); M. Kohmoto, Ann. Phys. (N.Y.) **160**, 343 (1985).
[24] X. Cai, S. Chen, and Y. Wang, Phys. Rev. A **83**, 043613 (2011).
[25] P. Streda, J. Phys. C **15**, L717 (1982).
[26] M. Rigol, Phys. Rev. A **72**, 063607 (2005).
[27] Q. Zhou and T. L. Ho, Phys. Rev. Lett. **105**, 245702 (2010).
[28] M. Köhl, H. Moritz, T. Stöferle, K. Günter, and T. Esslinger, Phys. Rev. Lett. **94**, 080403 (2005).